RESEARCH ARTICLE

Magnetic Resonance in Medicine

Hybrid algorithms for SAR matrix compression and the impact of post-processing on SAR calculation complexity

Stephan Orzada[1] | Thomas M. Fiedler[1] | Mark E. Ladd[1,2,3,4]

[1]Medical Physics in Radiology, German Cancer Research Center (DKFZ), Heidelberg, Germany

[2]Erwin L. Hahn Institute for MRI, University Duisburg-Essen, Essen, Germany

[3]Faculty of Physics and Astronomy, Heidelberg University, Heidelberg, Germany

[4]Faculty of Medicine, Heidelberg University, Heidelberg, Germany

Correspondence
Stephan Orzada, German Cancer Research Center (DKFZ), Im Neuenheimer Feld 280, 69120 Heidelberg, Germany.
Email: stephan.orzada@dkfz.de

Abstract

Purpose: This study proposes faster virtual observation point (VOP) compression as well as post-processing algorithms for specific absorption rate (SAR) matrix compression. Furthermore, it shows the relation between the number of channels and the computational burden for VOP-based SAR calculation.

Methods: The proposed new algorithms combine the respective benefits of two different criteria for determining upper boundedness of SAR matrices by the VOPs. Comparisons of the old and new algorithms are performed for head coil arrays with various channel counts. The new post-processing algorithm is used to post-process the VOP sets of nine arrays, and the number of VOPs for a fixed median relative overestimation is compared.

Results: The new algorithms are faster than the old algorithms by a factor of two to more than 10. The compression efficiency (number of VOPs relative to initial number of SAR matrices) is identical. For a fixed median relative overestimation, the number of VOPs increases logarithmically with the number of RF coil channels when post-processing is applied.

Conclusion: The new algorithms are much faster than previous algorithms. Post-processing is very beneficial for online SAR supervision of MRI systems with high channel counts, since for a given number of VOPs the relative SAR overestimation can be lowered.

KEYWORDS
local, MRI, SAR, specific absorption rate, virtual observation points, VOP compression, VOPs

1 | INTRODUCTION

Driven by the benefits of the super-linear increase in SNR,[1,2] there has been a constant push toward higher magnetic field strengths in MRI. While systems with a main magnetic field strength of 7T have recently been approved for clinical use, a human MRI system with a field strength of 14T is being built in the Netherlands.[3]

While the increase in SNR is beneficial, ultra-high field strengths have the drawback of wave effects in the excitation fields.[4,5] To counter these effects, a multitude of different transmit methods have been proposed. Examples for these are RF shimming,[6,7] kT-points,[8] 2D spokes,[9] 3D tailored radiofrequency pulses,[10] Transmit SENSE,[11,12] and TIAMO.[13] One thing all of these different methods

have in common is the use of multi-channel transmit arrays to influence the B_1^+ distribution by the superposition of the fields from all coils/antennas with different amplitudes and phases. It is important to note that of course the electric fields also vary with the different amplitudes and phases, leading to a different distribution of specific absorption rate (SAR) for each set of amplitudes and phases. Thus, both global and locally averaged SAR are now functions of the complex excitation vector, and not simply a function of total input power as in single-channel transmit systems. The regulatory guidelines[14] set limits for local, partial body, head, and whole-body SAR aspects that must not be exceeded during an MRI exam.

It is not possible to measure SAR in vivo. Therefore, simulations in realistic body models are required to obtain information on the field distribution within the body.[15] From these simulations, SAR matrices can be computed,[16] which contain information on the fields and tissue within a certain volume of the model. Using a vector–matrix–vector multiplication of a SAR matrix with the excitation vector, the SAR value of a volume can easily be calculated. This framework can be used for SAR-constrained pulse calculation as well as for online supervision.

The guideline requires that every mesh cell within the body model forms the center of an averaging volume[17]; therefore, the number of local SAR matrices for a single model can be on the order of 10^6 or even 10^7, requiring a huge computational effort and preventing real-time SAR supervision. Fortunately, compression algorithms have been proposed that trade the number of SAR matrices for an overestimation of SAR. The first algorithm was proposed by Eichfelder and Gebhardt in 2011.[18] This algorithm clusters the matrices around so-called virtual observation points (VOPs), where for any excitation vector a VOP provides a SAR value higher than that of any SAR matrix in the respective cluster. In 2012 Lee et al. presented an improved non-clustering algorithm,[19] where the VOPs jointly upper bound all matrices. While this algorithm achieves much better compression, it is computationally very demanding. In 2017, Kuehne et al. presented an improvement that speeds up the algorithm of Lee et al. by a large factor.[20] Orzada et al. found in 2021 that the speed and compression efficiency could further be improved by iteratively restarting the algorithm of Lee et al. including Kuehne et al.'s enhancement, with a reduced overestimation at each iteration step.[21] Furthermore, Orzada et al. introduced a post-processing algorithm based on Lee et al.'s criterion for upper bounding that could decrease the overestimation for a given set of VOPs,[22] while keeping the number of VOPs constant. A compression with low overestimation is important, because overestimation on the order of several hundred percent has been shown to occur for high channel counts.[23]

Recently, Gras et al. published a new criterion for checking whether a SAR matrix is upper bounded by the set of VOPs.[24] While the number of unknowns in the criterion of Lee et al. (designated convex combination [CC] in the following) is equal to the number of VOPs in the set, the number of unknowns in the criterion of Gras et al. (designated convex optimization [CO] in the following) is two times the number of channels. Gras et al. could show that the CO criterion leads to a shorter computation time when the number of VOPs is large, while the compression efficiency is identical.

In light of the large number of VOPs necessary for low overestimation at high transmit channel counts,[25] it is important to have fast algorithms, especially for very large models. In this work, we present new algorithms for compression and post-processing that combine CO and CC to increase the calculation speed both at low and high numbers of VOPs. With the improved calculation speed of the post-processing algorithm, we furthermore are now able to show its impact on SAR calculation complexity.

2 | METHODS

First, we would like to provide a brief overview of the two criteria CC and CO used in this work in a unified notation. In the following, $\mathbf{S}_v$ denotes an SAR matrix from the full set of SAR matrices V_{full}, while $\tilde{\mathbf{S}}_w$ denotes a matrix from the set of VOPs V_{sub}, and $\mathbf{D}$ denotes the overestimation matrix. All matrices are Hermitian matrices of size N_c by N_c, with N_c being the number of channels.

The CC criterion introduced by Lee et al.[19] can be written as follows:

$$\mathrm{r}_{CC}(\mathbf{S}_v) = \max_{c_{w,v}} \lambda_{\min}\left(\sum_{w \in V_{sub}} \left(c_{w,v}\tilde{\mathbf{S}}_w\right) + \mathbf{D} - \mathbf{S}_v\right)$$
$$\text{with } \sum_w c_{w,v} = 1 \wedge c_{w,v} \in [0,1]. \quad (1)$$

where $c_{w,v}$ are real valued scalars and $\lambda_{\min}(\mathbf{M})$ denotes the minimum eigenvalue of the matrix $\mathbf{M}$. If $\mathrm{r}_{CC}(\mathbf{S}_v) \geq 0$, the set of VOPs dominates the matrix $\mathbf{S}_v$ meaning that the set of VOPs has a higher SAR value for any given excitation vector. If $\mathrm{r}_{CC}(\mathbf{S}_v) < 0$, the matrix is not dominated and needs to be included in the set of VOPs. This is an optimization problem where the number of unknowns is equal to the number of VOPs.

Kuehne et al.[20] showed that it is not necessary to use the CC criterion on all matrices $\mathbf{S}_v$ directly. When a feasible solution for one matrix $\mathbf{S}_q$ has been found, a matrix

$\mathbf{P}_q = \sum_{w \in V_{sub}} (c_{w,q} \tilde{\mathbf{S}}_w) + \mathbf{D}$ can be formed. This can be used to calculate.

$$r_{CCK}(\mathbf{S}_v) = \lambda_{\min}(\mathbf{P}_q - \mathbf{S}_v) \text{ with } v \in V_{full}. \quad (2)$$

If $r_{CCK}(\mathbf{S}_v) \geq 0$, the set of VOPs dominates the matrix $\mathbf{S}_v$. Since this step does not include an optimization, it is much faster than using CC directly. $r_{ccK}(\mathbf{S}_v) \geq 0$ can either be calculated by eigenvalue calculation, or by using Cholesky factorization, since we are not interested in the actual value, but only in the decision whether it is above or below zero. It should be noted here that the coefficients $c_{w,q}$ can be calculated for any matrix $\mathbf{S}$ regardless of whether it is an element of V_{full} or not. In any case, $r_{CCK}(\mathbf{S}_v) \geq 0$ means that the set of VOPs dominates the matrix $\mathbf{S}_v$.[24]

The CO criterion introduced by Gras et al.[24] is a more direct approach to the problem, as it calculates the ratio of the SAR from the SAR matrix under test $\mathbf{S}_v$ divided by the maximum of the SAR over the VOPs $\tilde{\mathbf{S}}$ over complete excitation space:

$$r_{CO}(\mathbf{S}_v) = \max_{\mathbf{x} \in \mathbb{C}^{N_c} - \{0\}} \left(\left(\max_{\mathbf{S}_w \in V_{sub}} (\mathbf{x}^H (\tilde{\mathbf{S}}_w + \mathbf{D}) \mathbf{x}) \right)^{-1} \mathbf{x}^H \mathbf{S}_v \mathbf{x} \right) \quad (3)$$

Here $\mathbf{x}$ is the complex valued excitation vector with N_c elements. If $r_{CO}(\mathbf{S}_v) \leq 1$, $\mathbf{S}_v$ is dominated by the set of VOPs.

To make this feasible for optimization, Gras et al. reformulated this problem as.

$$r_{CO}(\mathbf{S}_v) = \max_{\mathbf{x} \in \mathbb{R}^{2N_c}} (\mathbf{x}^T \mathbf{S}_{v,\mathbb{R}} \mathbf{x}) \text{ subject to}$$
$$\mathbf{x}^T (\tilde{\mathbf{S}}_{w,\mathbb{R}} + \mathbf{D}_{\mathbb{R}}) \mathbf{x} \leq 1, \forall \mathbf{S}_w \in V_{sub} \quad (4)$$

with

$$\tilde{\mathbf{S}}_{w,\mathbb{R}} = \begin{pmatrix} \mathscr{R}(\tilde{\mathbf{S}}_w) & -\mathscr{I}(\tilde{\mathbf{S}}_w) \\ \mathscr{I}(\tilde{\mathbf{S}}_w) & \mathscr{R}(\tilde{\mathbf{S}}_w) \end{pmatrix} \text{ and } \mathbf{D}_{\mathbb{R}} = \begin{pmatrix} \mathscr{R}(\mathbf{D}) & -\mathscr{I}(\mathbf{D}) \\ \mathscr{I}(\mathbf{D}) & \mathscr{R}(\mathbf{D}) \end{pmatrix}. \quad (5)$$

Eq. (3) has an infinite number solutions, since the vector $\mathbf{x}$ can be multiplied by any complex scalar other than 0 without changing the result. Eq. (4) still has an infinite number of optima since the complex $\mathbf{x}$ can be multiplied by any complex scalar with an absolute value of 1 without changing the result. This can be problematic for the convergence of gradient based optimizers. Therefore, in our work we change the calculation of r_{CO} by fixing the imaginary part of the last channel to 0:

$$r_{CO}(\mathbf{S}_v) = \max_{\mathbf{x} \in \mathbb{R}^{2N_c}} (\mathbf{x}^T \mathbf{S}_{v,\mathbb{R}} \mathbf{x}) \text{ subject to}$$
$$\mathbf{x}^T (\tilde{\mathbf{S}}_{w,\mathbb{R}} + \mathbf{D}_{\mathbb{R}}) \mathbf{x} \leq 1, \forall \mathbf{S}_w \in V_{sub} \wedge \mathbf{x}_{2N_c} = 0 \quad (6)$$

This only has a single optimum.

An important difference between the two criteria is the fact that for the CC criterion, the optimization has to prove that the matrix under test is dominated by the set of VOPs, while for the CO criterion the optimization has to prove that the matrix under test is not dominated. This means that if the optimization for some reason fails to converge for the CC criterion, an unnecessary matrix is added to the VOPs, reducing the compression. Failing to converge with the CO criterion leads to a necessary matrix not being included in the set of VOPs, leading to a potentially unsafe set of VOPs.

Another difference between the two criteria is computational effort. In the case of the CO criterion, the number of unknowns is two times the number of channels minus one, so in difference to the CC criterion, the number of unknowns is constant throughout the process of compression, only the number of boundary conditions increases. On the other hand, each matrix $\mathbf{S}_v$ has to be tested by an optimization, whereas when using the CC criterion, only a fraction of the matrices has to be tested directly as explained above. In our proposed hybrid algorithm we use these different properties of the criteria to our advantage.

2.1 | Proposed hybrid compression algorithm

In the following we will designate the hybrid algorithm "criteria hybrid" (CH) and its iterative form iCH.

Figure 1 shows a simplified flow chart of the proposed algorithm that uses the iterative approach presented in,[21] where the compression is restarted with a lower overestimation and the set of VOPs from the previous iteration. All SAR matrices are sorted by their respective highest eigenvalue in a descending order. In difference to previous implementations of CC,[20,21] the first set of coefficients is not calculated for the first SAR matrix in the sorted set, but for the mean of all SAR matrices. Regardless of whether this mean matrix is dominated or not, the coefficients are subsequently used to check all matrices of the set with Eq. (2) as described by Kuehne et al. in.[20] This part is marked with a green A in the flow chart. Please note that this mean matrix is not included in the VOPs. This step is only used to find a large number of matrices that are dominated by the already existing set of VOPs. The matrices that exit block A are all matrices from the full set of SAR matrices that have not already been found to be dominated.

As long as the number of VOPs is 30 or lower, the CC criterion with the enhancement of Kuehne et al. is used, exactly as described by Orazda et al.[21] This part is marked

FIGURE 1 Simplified flow chart of the proposed compression algorithm. The main parts of the algorithm are labeled with green A, B, and C. (A) The new pre-check where the mean of all matrices is used instead of the matrix with the highest eigenvalue. (B) The algorithm using the CC criterion as it was implemented previously, but without a stopping criterion. (C) Our implementation of the CO criterion with a block wise check instead of checking all remaining matrices at once. CC, convex combination; CO, convex optimization; SAR, specific absorption rate.
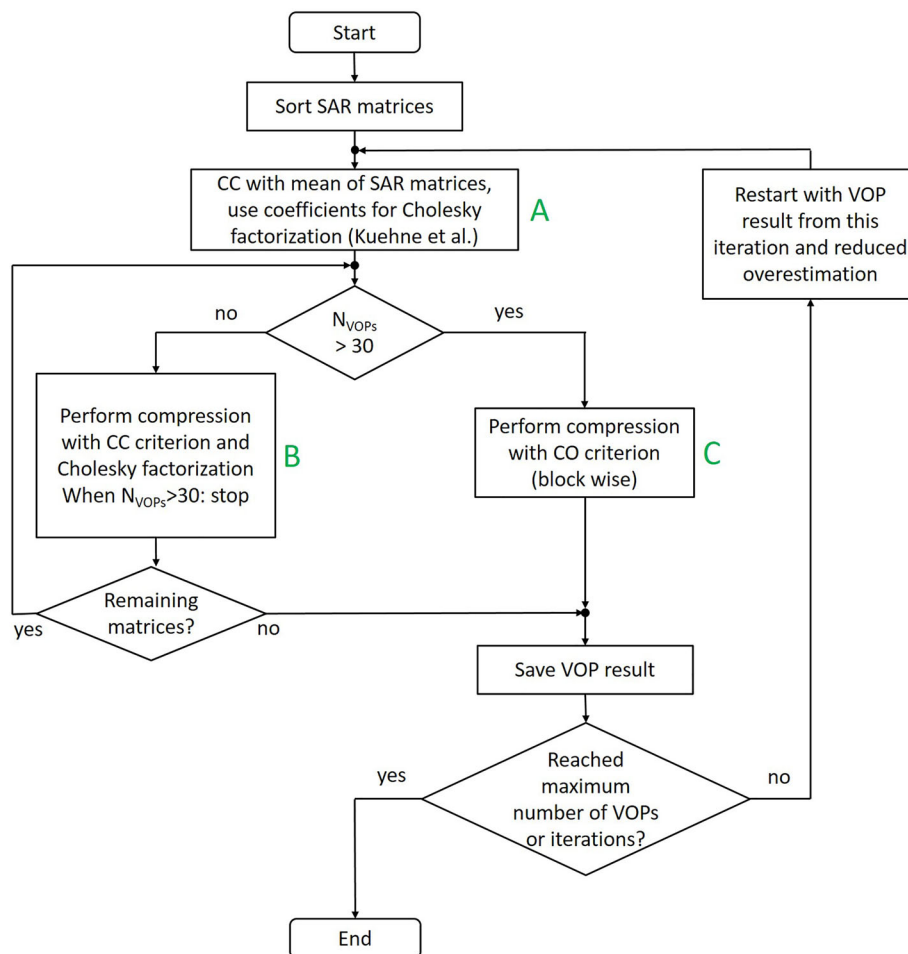
with a green B in the flow chart. At least for the investigated number of channels in this paper and in,[24] 30 VOPs seems to be the point where CC and CO exhibit approximately the same computational burden. As soon as the number of 30 VOPs is reached, this calculation is stopped. If there are remaining matrices, these are checked with the CO criterion (marked with a green C in the flow chart), as is described in the following.

In the first step of using the CO criterion, all remaining SAR matrices (coming either from the part marked by the green B or green A) are checked for domination with the CO criterion, as proposed by Gras et al.[24] All dominated matrices are dropped; the remaining matrix with the highest eigenvalue is added to the set of VOPs. In all further steps within the compression with the CO criterion, a block of 10 000 matrices is checked with the CO criterion. For a block of size N, the first N matrices of the remaining sorted SAR matrices are used. All dominated matrices are dropped and the non-dominated matrix with the highest eigenvalue is added to the VOPs. The block size is adapted by multiplying 10 000 by the ratio of dominated matrices over the current block size. This step is repeated until all SAR matrices are dominated. Note that this is

equivalent but not identical to the algorithm proposed by Gras et al.[24] Gras et al. check all remaining matrices. This leads to matrices that are not dominated being unnecessarily checked repeatedly. With the block-wise check, the number of repeated checks is decreased and the computational burden reduced. To provide an example of why this is the case, let us assume an iteration step that starts with 50 VOPs and finishes with 100 VOPs. A matrix with a comparatively low maximum eigenvalue that is only dominated by the final set of VOPs will be checked 50 times in the original implementation of the code, as all remaining matrices are checked every time a new VOP is added to the set. In our block wise implementation, it will only be checked during the very first run and when it is finally included in a block. Ideally only two checks are necessary.

When all matrices have been checked, the result is saved, the overestimation is reduced, and the compression is restarted if the maximum number of VOPs or iterations has not yet been reached. Upon each restart, the full set of SAR matrices is restored to be checked against the VOPs from the previous run, but now with a reduced overestimation.

In the Matlab implementation, code for the CO criterion written by Gras et al.[24] was used with improvements implemented as stated above.

2.2 | Proposed post-processing algorithm

The proposed post-processing algorithm (PP-CH) shares most steps with the algorithm presented by Orzada et al. in[22] (PP-CC).

After sorting of all the SAR matrices, the CC criterion is used to calculate coefficients to dominate the mean of all SAR matrices using the already present set of VOPs. Regardless of whether this matrix can be dominated or not, the coefficients obtained are used to check whether any of the SAR matrices can be dominated by the set of VOPs, as proposed by Kuehne et al.[20] All dominated matrices are dropped. Just like in the compression algorithm described above, this leads to a quick reduction in overall matrix count.

In the following, Step 2 from the algorithm in[22] is performed differently. Instead of employing the CC criterion, the CO criterion is used in the new algorithm. For speed-up, a block of 400 matrices was checked, the dominated matrices were dropped, and the largest, non-dominated matrix was used for the further steps. Step 6 from[22] is not used. It should be noted that the CC criterion is still used in Step 3, as it is necessary for calculation of the individual overestimation added to each VOP.

The algorithm is now as follows:

1. Sort matrices in V_{full} according to their highest respective eigenvalue (ascending) and set all overestimation matrices $\mathbf{D}_w$ to zero matrices.
2. Calculate the coefficients $c_{w,q}$ for the mean of all matrices and then calculate r_{CCK}. Delete all dominated matrices from V_{full}.
3. By calculating r_{CO} for the first 400 matrices of V_{full} in parallel, check for domination. It is important to note that in this step the VOPs $\tilde{\mathbf{S}}_w$ are used with their respective overestimation matrices $\mathbf{D}_w$. The dominated matrices are deleted from V_{full}. Repeat until a matrix is found that is not dominated. The first matrix found that is not dominated is set as the current matrix $\mathbf{S}_v$ and the algorithm proceeds to step 4.
4. Find $c_{w,v}$ to maximize the minimum eigenvalue of $\mathbf{P} = \sum_{w \in V_{sub}} c_{w,v} \tilde{\mathbf{S}}_w - \mathbf{S}_v$.
5. Calculate $\mathbf{Z}$ that fulfills $\mathbf{P} = \sum_{w \in V_{sub}} c_{w,v} \tilde{\mathbf{S}}_w + \mathbf{Z} - \mathbf{S}_v$ is PSD.
6. Update all $\mathbf{D}_w$ by finding a $\mathbf{Z}_w$ such that $\mathbf{P}_w = \mathbf{D}_w + \mathbf{Z}_w - \mathbf{Z}\left(\frac{c_{wv}}{\sum_w c_{wv}^2}\right)$ is PSD.
7. Iterate steps 3–5 until all matrices are dominated.

2.3 | Numerical experiments

Two different SAR matrix sets were used: The SAR matrices of the 8-channel and 24-channel head arrays from[25] with 1.77e6 matrices and 1.87e6 matrices, respectively. For the both head arrays, the body model was truncated below the shoulders.

Calculations were performed on a virtual workstation with 40 CPU cores (AMD EPYC-Milan @ 2.8GHz, Advanced Micro Devices, Inc., Santa Clara, CA, USA), 256 GB of RAM, and a GPU with 20 GB of RAM (one half of an A100 GPU, NVIDIA Corp., Santa Clara, CA, USA).

All algorithms in this paper were implemented in Matlab (The Mathworks, Inc., Natick, MA, USA).

Three different compression algorithms were compared:

1. "iCC": The algorithm by Orzada et al.[21] in the version "Compression with VOPID and Timings", https://sourceforge.net/projects/enhanced-sar-compression/
2. "iCO": The algorithm presented by Gras et al.,[24] https://github.com/VincentGras/VOPcompressionCO (Commit 66378c1)
3. "iCH" The hybrid Algorithm presented in this paper, https://github.com/sOrzada/VOP_Compression (Commit 59d53e4)

The 8- and 24-channel datasets were used in speed tests for all algorithms. All three algorithms were started with the same overestimation. The overestimation reduction factor was $R = \sqrt{2}$. Although all algorithms have pure CPU versions available, GPU versions of the algorithms were used where applicable.

Two different post-processing algorithms were compared:

1. "PP-CC": The algorithm presented by Orzada et al.[22]: https://sourceforge.net/projects/vop-post-processing/
2. "PP-CH": The algorithm presented in this paper. https://github.com/sOrzada/VOP_Compression

The 8- and the 24-channel datasets were used to compare the two post-processing algorithms.

Furthermore, the supervision complexity was investigated using the PP-CH post-processing algorithm. SAR matrices for 9 head coils with 4–24 channels from Orzada et al.[25] were compressed with the proposed iCH VOP algorithm starting at 40% of worst-case local SAR for the overestimation. With each iteration step, the overestimation was reduced by division by the third root of two to provide additional datapoints for interpolation versus

$\sqrt{2}$. A total of 12 iteration steps were calculated for each array. Afterward, each VOP set was post-processed with the PP-CH algorithm. The median relative overestimation of 1e6 random excitation vectors was calculated for all VOP sets with and without post-processing. To calculate the number of VOPs for identical median overestimation, a linear interpolation was used on the logarithmized data for number of VOPs versus median relative overestimation.

3 | RESULTS

3.1 | Hybrid compression algorithm

Timing results for the compression of the 8-channel dataset can be found in Figure 2. As shown by Gras et al., the iCO algorithm is faster than iCC for VOP counts above 100 (Figure 2A). The proposed iCH algorithm is faster than both of the other algorithms apart from the first point where iCC and iCH are identical. The small difference in

timing most probably results from different loading times of the dataset from a network storage with varying traffic. There is a very slight difference in the number of VOPs visible between the different algorithms. This can in part be attributed to numerical precision. When eigenvalues are close to 0, eigenvalue decomposition and Cholesky factorization, for example, can come to different results concerning the definiteness of SAR matrices. Figure 2B shows the speed-up factor for the iCH compression algorithm without post-processing versus the other algorithms. With an increasing number of VOPs, the speed-up in comparison to iCC increases rapidly, reaching more than 400 at ~340 VOPs. The speed-up factor of the iCH algorithm versus iCO slightly decreases with the number of VOPs, but still is more than 2 at ~340 VOPs.

Figure 2C,D show timings for the iterations finishing with ~70 and ~340 VOPs, respectively. It is visible that the CC criterion with subsequent checks with Cholesky factorization quickly finds many upper-bounded matrices in the first step in this iteration. Thereafter, the CC criterion takes much longer to test the remaining matrices and add new
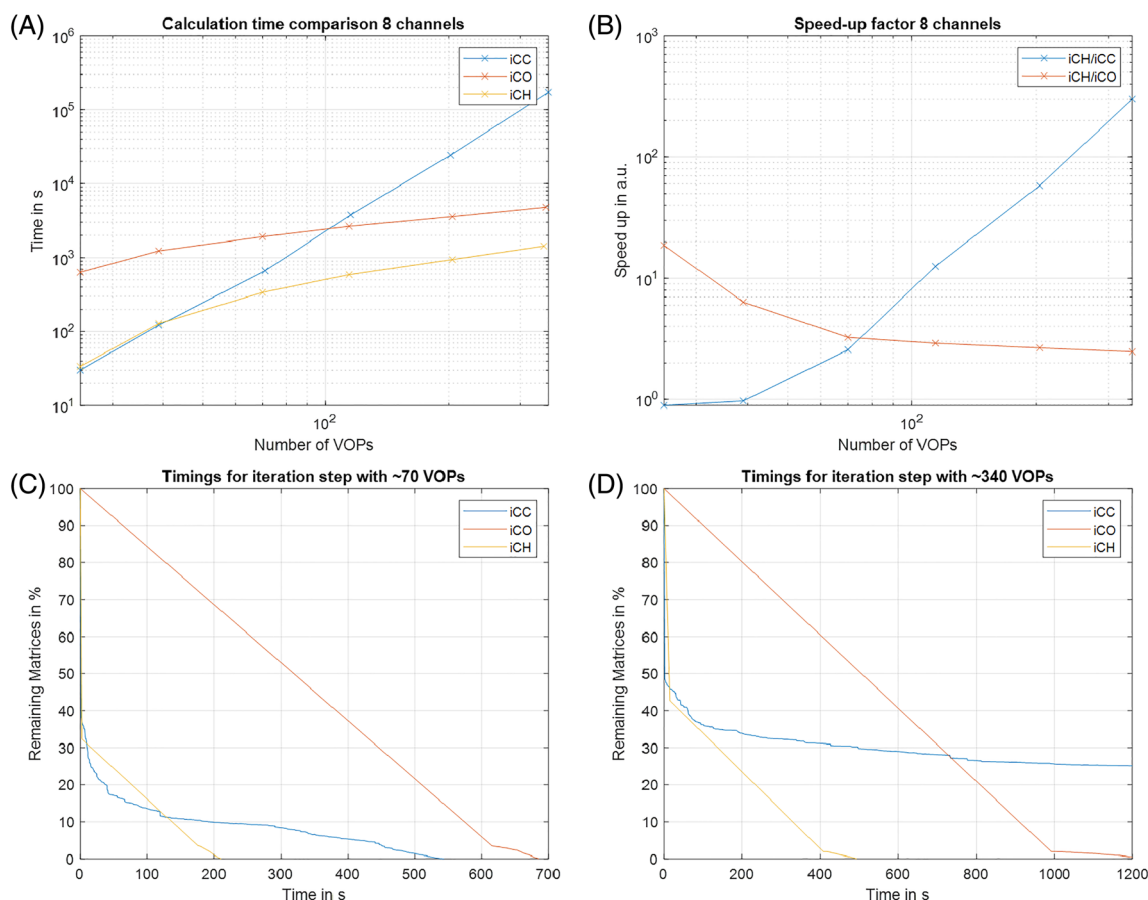

FIGURE 2 Timing results for the compression of the eight-channel dataset. (A) Calculation time versus number of virtual observation points (VOPs) for the three different algorithms. (B) Speed-up factor for the hybrid compression algorithm without post-processing compared to the two other algorithms. (C, D) Percentage of remaining matrices versus time for the three different algorithms for the iteration steps finishing with ~70 and ~340 VOPs, respectively.
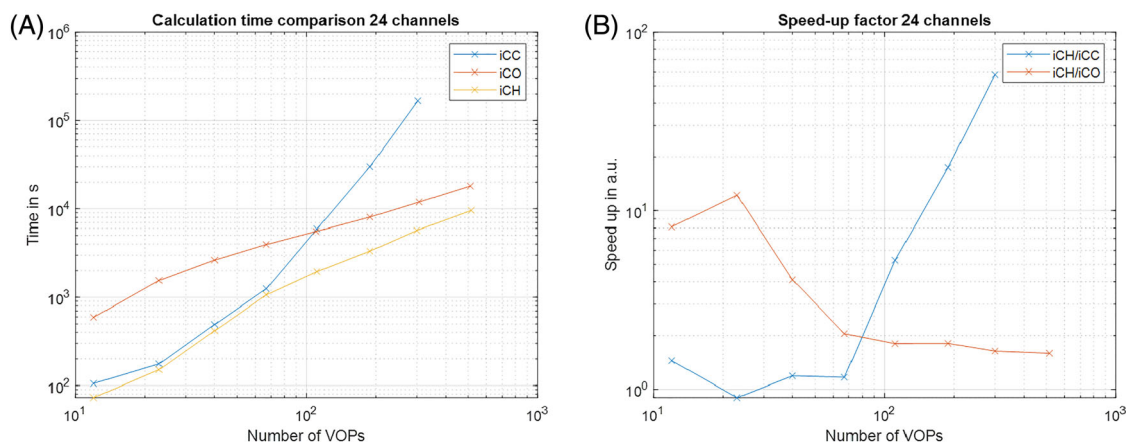
FIGURE 3 Timing results for the compression of the 24-channel dataset. (A) Calculation time versus number of virtual observation points (VOPs) for the three different algorithms. (B) Speed-up factor for the hybrid compression algorithm without post-processing compared to the two other algorithms.

VOPs to the sub-volume than what can be achieved with the CO criterion. Furthermore, it can be seen that using the CC criterion on the mean of all SAR matrices removes more matrices than using the SAR matrix with the highest eigenvalue. It is also visible that with a higher number of VOPs, the number of matrices found to be upper-bounded in this first step is reduced, slightly reducing the speed advantage of the iCH algorithm. Another thing that can be seen from these plots is the effectiveness of the block-wise calculation of the CO criterion with variable block size, especially after 90 and 300 s, when the number of repeated checks of matrices is reduced by the block-wise calculation in comparison to checking all remaining matrices as implemented by Gras et al.

The results for the 24-channel dataset are shown in Figure 3. Again, the iCH algorithm outperforms both of the other algorithms. The timing difference in the first point can again be attributed to different loading times of the dataset from the network drive.

3.2 | Hybrid post-processing algorithm

Timing comparisons for the new and old versions of the post-processing algorithm can be viewed in Figure 4A for the eight-channel dataset and Figure 4B for the 24-channel dataset. The new algorithm is visibly faster: at 50–70 VOPs the speed enhancement exceeds an order of magnitude. For the original algorithm, VOP sets with more than 70 VOPs were not used due to the expected long calculation times.

Figure 4C,D show the median overestimation comparison for the VOP sets obtained with compression only (iCH) and post-processed VOPs (PP-CH) for the 8-channel and 24-channel datasets, respectively. It is notable that the

post-processing is more effective for the dataset with more channels.

3.3 | Impact of post-processing on calculation complexity

Figure 5 shows the number of VOPs versus the median relative overestimation for 4 to 24 channels in a double logarithmic plot. Figure 5A shows the results after compression with the iCH algorithm only, while Figure 5B shows the results for the same VOP sets after post-processing. Above approximately 50 VOPs, the relationship between the logarithm of the median relative overestimation and the logarithm of the number of VOPs appears linear. Furthermore, all line plots for different channel counts appear to run parallel to one another. When comparing the two plots, it is noticeable that the lines for higher channel counts are closer together for the post-processed VOPs.

From the above results, the number of VOPs for 10% median relative overestimation can be approximated by linear interpolation of the double logarithmized data. Figure 6 shows the number of VOPs from this interpolation versus the number of channels in a semi-logarithmic plot. A function $a + b \log N_{ch}$ can be fitted to the data with an adjusted R^2 of 0.98.

3.4 | Convergence of the CO criterion

When testing the compression results with the CO criterion as proposed by Gras et al.,[24] we noticed that $r_{CO}(\mathbf{S}_v)$ sporadically assumed values above 1 for the algorithms using the CO criterion. When this happened for a set of VOPs, it only happened for a few matrices of the full set
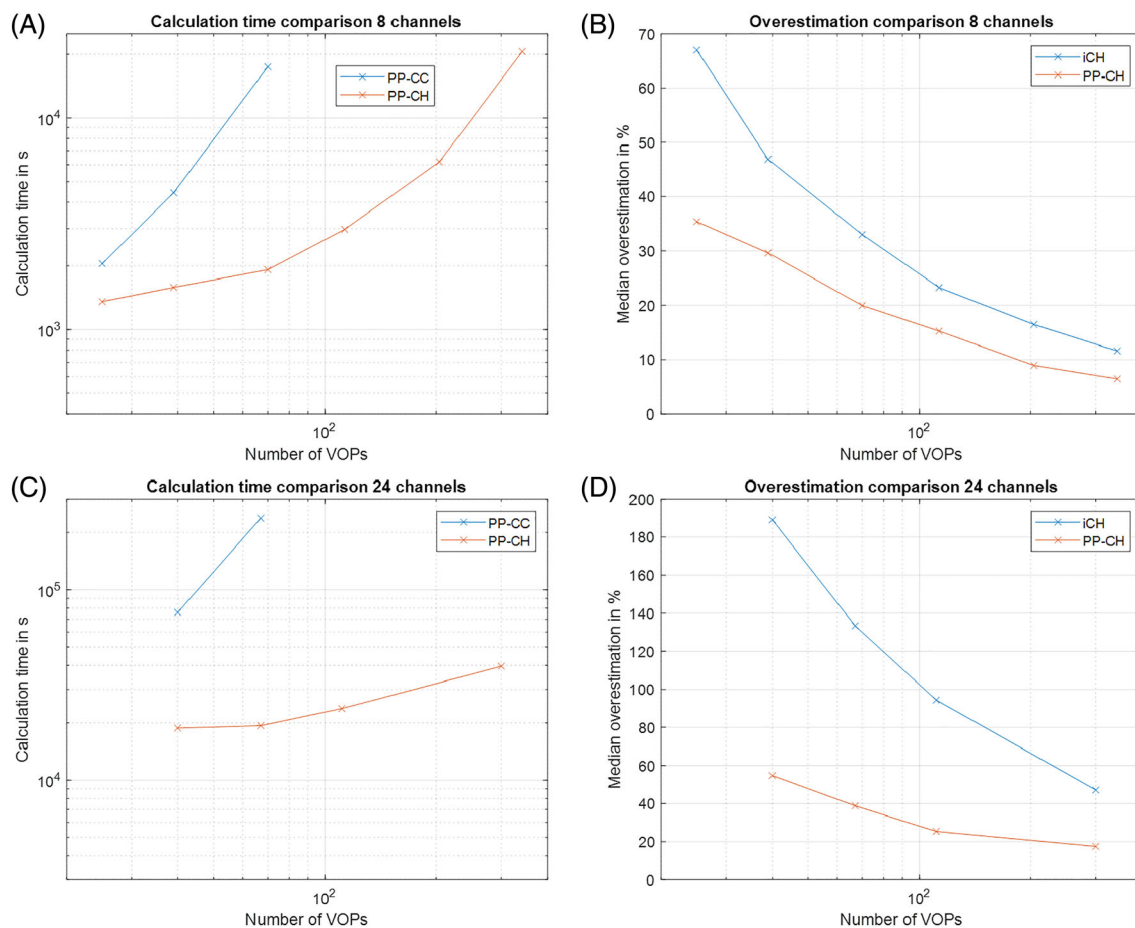
FIGURE 4 (A, B) show the calculation time comparison of the post-processing algorithms for the eight-channel and 24-channel datasets, respectively. It is visible that around 70 VOPs the older algorithm relying solely on CC takes more than 10 times longer than the new hybrid algorithm. (C, D) show the median overestimation before (iCH) and after (PP-CH) post-processing for the eight-channel and 24-channel datasets, respectively. It is notable that the reduction in overestimation is more pronounced for the dataset with more channels.
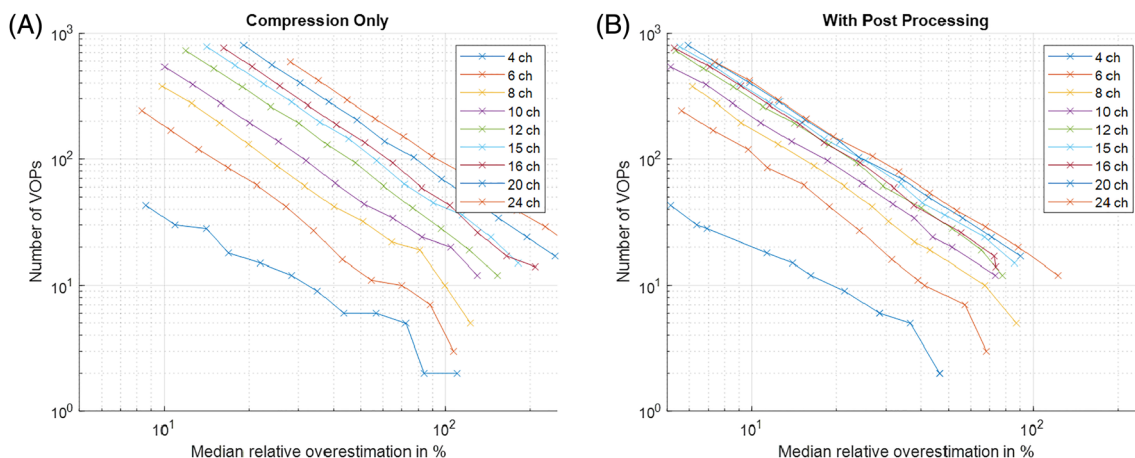

FIGURE 5 Number of virtual observation points (VOPs) versus median relative overestimation for 4 to 24 channels. (A) Results after compression with iCH. (B) Results after post-processing with the proposed hybrid post-processing algorithm. The four-channel result with post-processing only contains 10 instead of 12 results since the compression resulted in cases with an identical number of VOPs (2 VOPs and 6 VOPs). Please note that lower median relative overestimation is better.
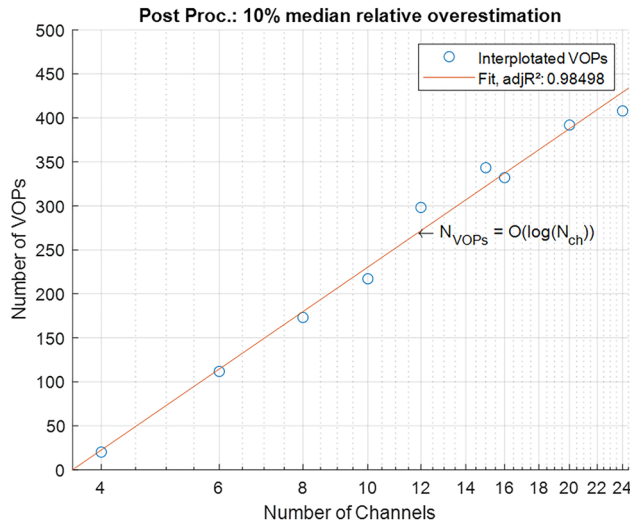
FIGURE 6 Number of virtual observation points (VOPs) versus number of channels for a fixed median relative overestimation of 10% after post-processing. The distribution can be well approximated by a logarithmic function $a + b \log N_{ch}$, with $a = -292.3$ and $b = 227$.

(<10) per model and the relative underestimation was below 1%. In the more than 200 million random test cases, we performed over all of the VOP sets in this work, no case of underestimation occurred. The occurrence of such underestimations could not be linked to the number of channels or number of VOPs. For example, while the check for the post-processed VOP set for the 24-channel array and 512 VOPs passed the test with a maximum $r_{CO}(\mathbf{S}_v)$ value of 0.9997, the VOP set of the 16-channel array with 764 VOPs failed the test with a maximum $r_{CO}(\mathbf{S}_v)$ value of 1.0035. This indicates that an underestimation of up to 0.35% can occur.

4 | DISCUSSION

The algorithm for compression of SAR matrices in this paper proved to be much faster than the previous algorithms for small as well as for large numbers of VOPs. At the same time, the compression efficiency is identical. Gras et al. mention in their paper that the CO criterion is the weaker criterion and therefore might offer higher compression in some cases.[24] Since the new hybrid algorithm (above a count of 30 VOPs) only uses the CC criterion to test which SAR matrices are already upper bounded, leaving the decision of which matrices are added to the VOP subset to the CO criterion, the hybrid algorithm should perform identically to the version published by Gras et al. Small differences in the number of VOPs can still occur due to numerical precision, but these are not safety relevant as the error is many orders of magnitude

lower than the actual SAR value. Although VOP compression itself is not normally time critical, since it is performed offline in advance of any real-time SAR monitoring, increased calculation speed is always appreciated; in special circumstances like the implementation of patient-specific SAR models[26] for SAR supervision, where the calculation needs to be performed online, increased speed might be a necessity.

The hybrid algorithm for post-processing presented in this paper is much faster than the previously presented algorithm.[22] At more than 70 VOPs for a 24-channel dataset, the speed increase is almost 100-fold. This speed increase allowed us to investigate the impact of the number of channels on the SAR calculation complexity after post-processing. While previous work showed an increase in the number of VOPs for a fixed median relative overestimation proportional to the number of channels to the power 2.3,[25] here we could show that the increase in the number of VOPs with post-processing is only on the order of the logarithm of the number of channels. Therefore, the increase in computational effort can be reduced from $\mathbf{O}(N_{ch}^{4.3})$ to $\mathbf{O}(N_{ch}^2 \log N_{ch})$, making the online supervision of systems with very high channel counts (≥ 64) much more feasible. This underscores the necessity to apply post-processing to VOPs, which has become much more feasible with the new algorithm, especially in the light of the arrival of high channel count systems.[27–29]

We furthermore found that VOPs with underestimation can result from using the CO criterion, independent of which algorithm is using the criterion. Even though we improved the convergence of the CO criterion by reducing the number of optima from a one-dimensional infinity to 1, increasing the number of iterations of the optimizer and reducing the tolerances, we still saw that the optimizer sporadically converges to different solutions depending on the starting vector. Fortunately, these underestimations are very small and the probability of encountering them during use of the VOP sets is very low, as we could not find any underestimation in more than 200 million random tests. Since the result from testing the VOP sets provides a relative factor for under- and overestimation, this could be corrected for by multiplying the VOP set with the result from the test.

5 | CONCLUSIONS

We have presented hybrid algorithms for SAR matrix compression and post-processing of VOP sets that are much faster than previous algorithms. Furthermore, with the faster post-processing algorithm, we could show that the increase in SAR calculation complexity with

the number of channels is much lower than previously reported when post-processing is used. These findings will facilitate online SAR supervision for very high channel counts.

DATA AVAILABILITY STATEMENT

The source Matlab source code for the algorithms introduced in this paper can be found on GitHub: https://github.com/sOrzada/VOP_Compression.

ORCID

Stephan Orzada https://orcid.org/0000-0001-9784-4354
Thomas M. Fiedler https://orcid.org/0000-0002-1556-375X

REFERENCES

1. Le Ster C, Grant A, Van de Moortele PF, et al. Magnetic field strength dependent SNR gain at the center of a spherical phantom and up to 11.7T. *Magn Reson Med*. 2022;88:2131-2138.
2. Pohmann R, Speck O, Scheffler K. Signal-to-noise ratio and MR tissue parameters in human brain imaging at 3, 7, and 9.4 tesla using current receive coil arrays. *Magn Reson Med*. 2016;75:801-809.
3. Bates S, Dumoulin SO, Folkers PJM, et al. A vision of 14 T MR for fundamental and clinical science. *Magma*. 2023;36:211-225.
4. Roschmann P. Radiofrequency penetration and absorption in the human body: limitations to high-field whole-body nuclear magnetic resonance imaging. *Med Phys*. 1987;14:922-931.
5. Van de Moortele PF, Akgun C, Adriany G, et al. B(1) destructive interferences and spatial phase patterns at 7 T with a head transceiver array coil. *Magn Reson Med*. 2005;54:1503-1518.
6. Collins CM, Liu W, Swift BJ, Smith MB. Combination of optimized transmit arrays and some receive array reconstruction methods can yield homogeneous images at very high frequencies. *Magn Reson Med*. 2005;54:1327-1332.
7. Metzger GJ, Snyder C, Akgun C, Vaughan T, Ugurbil K, Van de Moortele PF. Local B1+ shimming for prostate imaging with transceiver arrays at 7T based on subject-dependent transmit phase measurements. *Magn Reson Med*. 2008;59:396-409.
8. Cloos MA, Boulant N, Luong M, et al. kT-points: short three-dimensional tailored RF pulses for flip-angle homogenization over an extended volume. *Magn Reson Med*. 2012;67:72-80.
9. Setsompop K, Alagappan V, Gagoski B, et al. Slice-selective RF pulses for in vivo B1+ inhomogeneity mitigation at 7 tesla using parallel RF excitation with a 16-element coil. *Magn Reson Med*. 2008;60:1422-1432.
10. Saekho S, Yip CY, Noll DC, Boada FE, Stenger VA. Fast-kz three-dimensional tailored radiofrequency pulse for reduced B1 inhomogeneity. *Magn Reson Med*. 2006;55:719-724.
11. Grissom W, Yip CY, Zhang Z, Stenger VA, Fessler JA, Noll DC. Spatial domain method for the design of RF pulses in multicoil parallel excitation. *Magn Reson Med*. 2006;56:620-629.
12. Katscher U, Bornert P, Leussler C, van den Brink JS. Transmit SENSE. *Magn Reson Med*. 2003;49:144-150.
13. Orzada S, Maderwald S, Poser BA, Bitz AK, Quick HH, Ladd ME. RF excitation using time interleaved acquisition of modes (TIAMO) to address B1 inhomogeneity in high-field MRI. *Magn Reson Med*. 2010;64:327-333.
14. IEC. International Electrotechnical Commission (IEC). IEC 60601-2-33 Medical Electrical Equipment-Part 2-33: Particular Requirements for the Basic Safety and Essential Performance. 2022.
15. Fiedler TM, Ladd ME, Bitz AK. SAR simulations & safety. *Neuroimage*. 2018;168:33-58.
16. Zhu Y, Alon L, Deniz CM, Brown R, Sodickson DK. System and SAR characterization in parallel RF transmission. *Magn Reson Med*. 2012;67:1367-1378.
17. IEC/IEEE. International Electrotechnical Commission (IEC). IEC/IEEE 62704-1 Determining the peak spatial-average specific absorption rate (SAR) in the human body from wireless communications devices, 30 MHz to 6 GHz–Part 1: General requirements for using the finite-difference time-domain (FDTD) method for SAR calculations. 2017.
18. Eichfelder G, Gebhardt M. Local specific absorption rate control for parallel transmission by virtual observation points. *Magn Reson Med*. 2011;66:1468-1476.
19. Lee J, Gebhardt M, Wald LL, Adalsteinsson E. Local SAR in parallel transmission pulse design. *Magn Reson Med*. 2012;67:1566-1578.
20. Kuehne A, Waiczies H, Niendorf T. Massively accelerated VOP compression for population-scale RF safety models. *Proc Intl Soc Mag Reson Med*. 2017;25:478.
21. Orzada S, Fiedler TM, Quick HH, Ladd ME. Local SAR compression algorithm with improved compression, speed, and flexibility. *Magn Reson Med*. 2021;86:561-568.
22. Orzada S, Fiedler TM, Quick HH, Ladd ME. Post-processing algorithms for specific absorption rate compression. *Magn Reson Med*. 2021;86:2853-2861.
23. Fiedler TM, Orzada S, Floser M, et al. Performance analysis of integrated RF microstrip transmit antenna arrays with high channel count for body imaging at 7 T. *NMR Biomed*. 2021;34:e4515.
24. Gras V, Boulant N, Luong M, et al. A mathematical analysis of clustering-free local SAR compression algorithms for MRI safety in parallel transmission. *IEEE Trans Med Imaging*. 2023;43:722.
25. Orzada S, Akash S, Fiedler TM, Kratzer FJ, Ladd ME. An investigation into the dependence of virtual observation point-based specific absorption rate calculation complexity on number of channels. *Magn Reson Med*. 2023;89:469-476.
26. Homann H, Bornert P, Eggers H, Nehrke K, Dossel O, Graesslin I. Toward individualized SAR models and in vivo validation. *Magn Reson Med*. 2011;66:1767-1776.

27. Auerbach EJ, Delabarre L, Van de Moortele PF, et al. An integrated 32-channel transmit and 64-channel receive 7 tesla MRI system. *Proc Intl Soc Mag Reson Med.* 2017;25:1218.

28. Feng K, Hollingsworth NA, McDougall MP, Wright SM. A 64-channel transmitter for investigating parallel transmit MRI. *IEEE Trans Biomedical Engn.* 2012;59:2152-2160.

29. Orzada S, Solbach K, Gratz M, et al. A 32-channel parallel transmit system add-on for 7T MRI. *PLoS One.* 2019;14:e0222452.